REPORT No. 703

DESIGN CHARTS RELATING TO THE STALLING OF TAPERED WINGS

By H. A. Soulé and R. F. Anderson

SUMMARY

As an aid in airplane design, charts have been prepared to show the effects of wing taper, thickness ratio, and Reynolds number on the spanwise location of the initial stalling point. Means of improving poor stalling characteristics resulting from certain combinations of the variables have also been considered; additional figures illustrate the influence of camber increase to the wing tips, washout, central sharp leading edges, and wing-tip slots on the stalling characteristics. Data are included from which the drag increases resulting from the use of these means can be computed. The application of the data to a specific problem is illustrated by an example.

INTRODUCTION

In the investigation of the stalling of wings, a knowledge of the spanwise location of the initial stall and of the susceptibility to stalling of the tips is important because of the connection of these two factors with loss of damping in roll. A method of calculating the point along the span of tapered wings where stalling should begin was given in references 1 and 2. In a later report (reference 3), the method of references 1 and 2 was applied to an investigation of the optimum design of tapered wings, tip stalling being considered.

The present paper extends the previous work to a survey of tapered wings to determine the manner in which the spanwise location of the initial stall varies within the range of wing parameters covered by current design practice. For the guidance of designers, the results are presented in the form of charts for three Reynolds numbers, corresponding to three airplane sizes with wings having various taper ratios and root-thickness ratios. As in reference 3, the basic airfoil sections are the NACA 230 series. The wings were without flaps and had no sweep.

The various means considered of moving the stalling point inward were: increase of the percentage of camber of the airfoil sections from root to tip, washout, central sharp leading edges, and leading-edge tip slots. The effect of these methods of reducing the susceptibility of tip stalling on airplane performance is discussed. The use of the charts is illustrated by an example.

CALCULATION AND PRESENTATION OF THE DATA

CONDITIONS FOR THE CALCULATIONS

All the charts were obtained for unflapped wings having straight taper and rounded tips, as shown in figure 1, except for two special cases of a wing with a straight center section that will be discussed later. The taper ratio r is defined as c_s/c_t, where c_t and c_s are shown in figure 1. Taper ratios of 1, 2, and 5 were used.

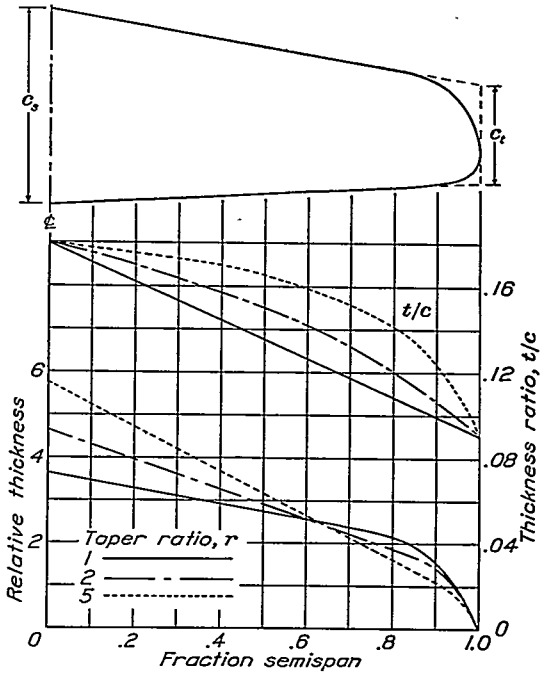

FIGURE 1.—Typical plan form and thickness variations.

The increase in camber of the airfoil sections from root to tip, when present, was linear. The camber is given as a percentage of the chord but will be referred to simply as "camber." Washout, when used, was also linear and was aerodynamic (angular difference between the zero-lift directions of the root and the tip sections). The NACA 230 series of airfoil sections was assumed for the wings without camber increase. For the cases with camber increase, the NACA 230 series sections were used at the root and the NACA 43009 section was used at the tips. The root thickness ratios were 0.12, 0.15, 0.18, and 0.21;

the tip thickness ratio was always 0.09. The thickness ratio is the maximum thickness t divided by the chord c. For all cases, the variation of the actual thickness along the span was linear. Typical variations of thickness and thickness ratio are shown in figure 1.

Three values of Reynolds numbers (4,000,000, 8,000,000, and 14,000,000), corresponding to the stalling speeds (without flaps) of three sizes of airplane, were considered. The Reynolds number was based on the mean chord, S/b. Typical airplanes corresponding to the three Reynolds numbers would have mean wing chords of 7, 12, and 18 feet and stalling speeds of 61, 71, and 81 miles per hour, respectively.

SPANWISE DISTRIBUTION OF LIFT COEFFICIENTS

Figures 2 and 3 present the distributions of section lift coefficients along the span that are necessary for the determination of the point at which stalling should start. Figure 2 gives the section lift coefficients $c_{l_{a1}}$ for wings without aerodynamic twist when the wing lift coefficient C_L is 1.0. For other wing lift coefficients, the section lift coefficients c_{l_a} are directly proportional to C_L and may be obtained from

$$c_{l_a}=C_L\, c_{l_{a1}}$$

Aerodynamic twist adds an increment of section lift

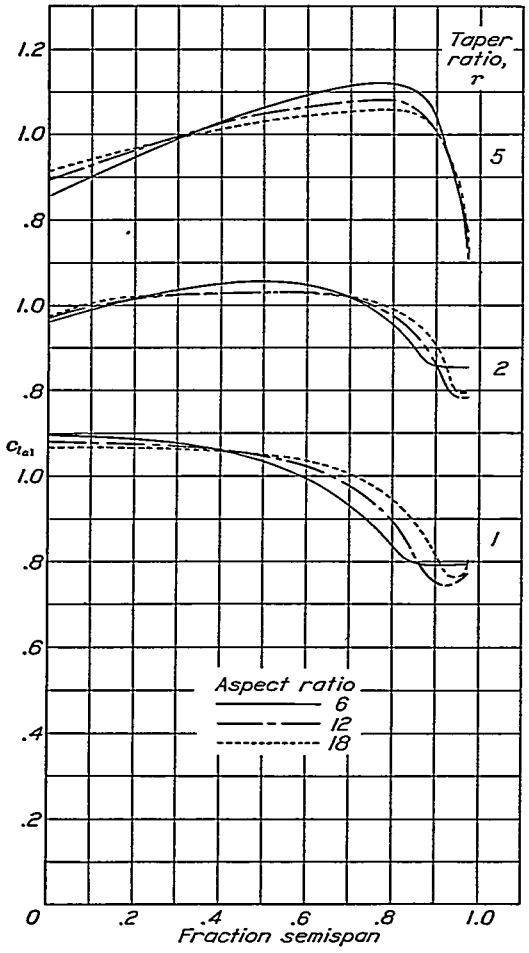

FIGURE 2.—Distribution of lift coefficient over semispan. No twist; C_L, 1.0.

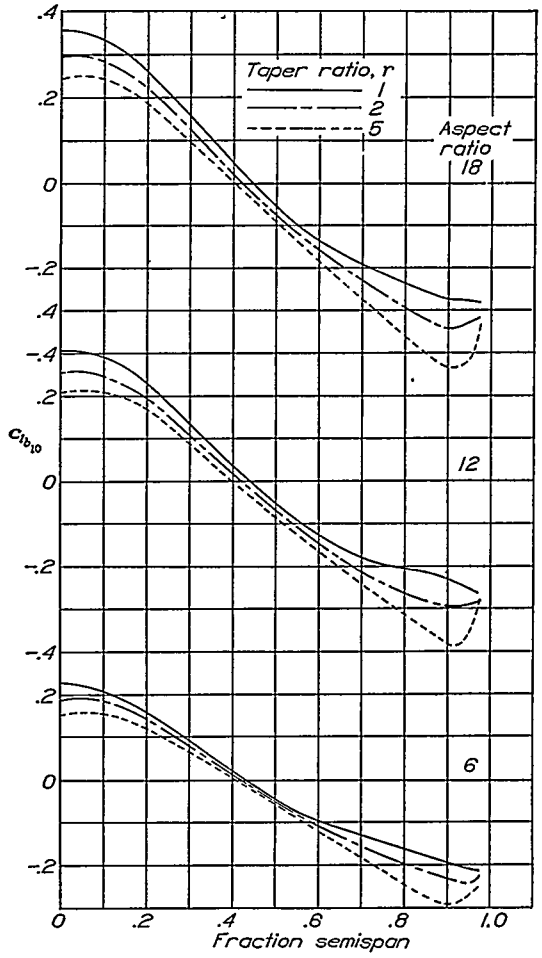

FIGURE 3.—Distribution of lift coefficient over semispan. 10° washout; C_L, 0; linear twist distribution.

coefficient c_{l_b} that is independent of the wing lift coefficient. Figure 3 gives section lift coefficients $c_{l_{b_{10}}}$ for wings with 10° washout at $C_L=0$. The effect of twist is directly proportional to the angle of twist and, for other values of the angle of twist ϵ, c_{l_b} is given by

$$c_{l_b}=-\frac{\epsilon}{10}\, c_{l_{b_{10}}}$$

where ϵ is in degrees and is negative for washout. In the general case, the section lift coefficient c_l may be written

$$c_l=c_{l_a}+c_{l_b}$$

When there is no twist, of course $c_{l_a}=c_l$.

Figures 2 and 3 are based on values from reference 1. The data in reference 1 can be used to determine the section lift coefficients for combinations of taper and aspect ratios other than shown in figures 2 and 3.

STALLING CHARTS

The calculated point along the span at which stalling should start is given in figures 4 and 5 for what may be called basic wings, that is, plain wings without washout or other means of moving the stalling point inward. The data are given for the three taper ratios, the four root thickness ratios, and the three Reynolds numbers.

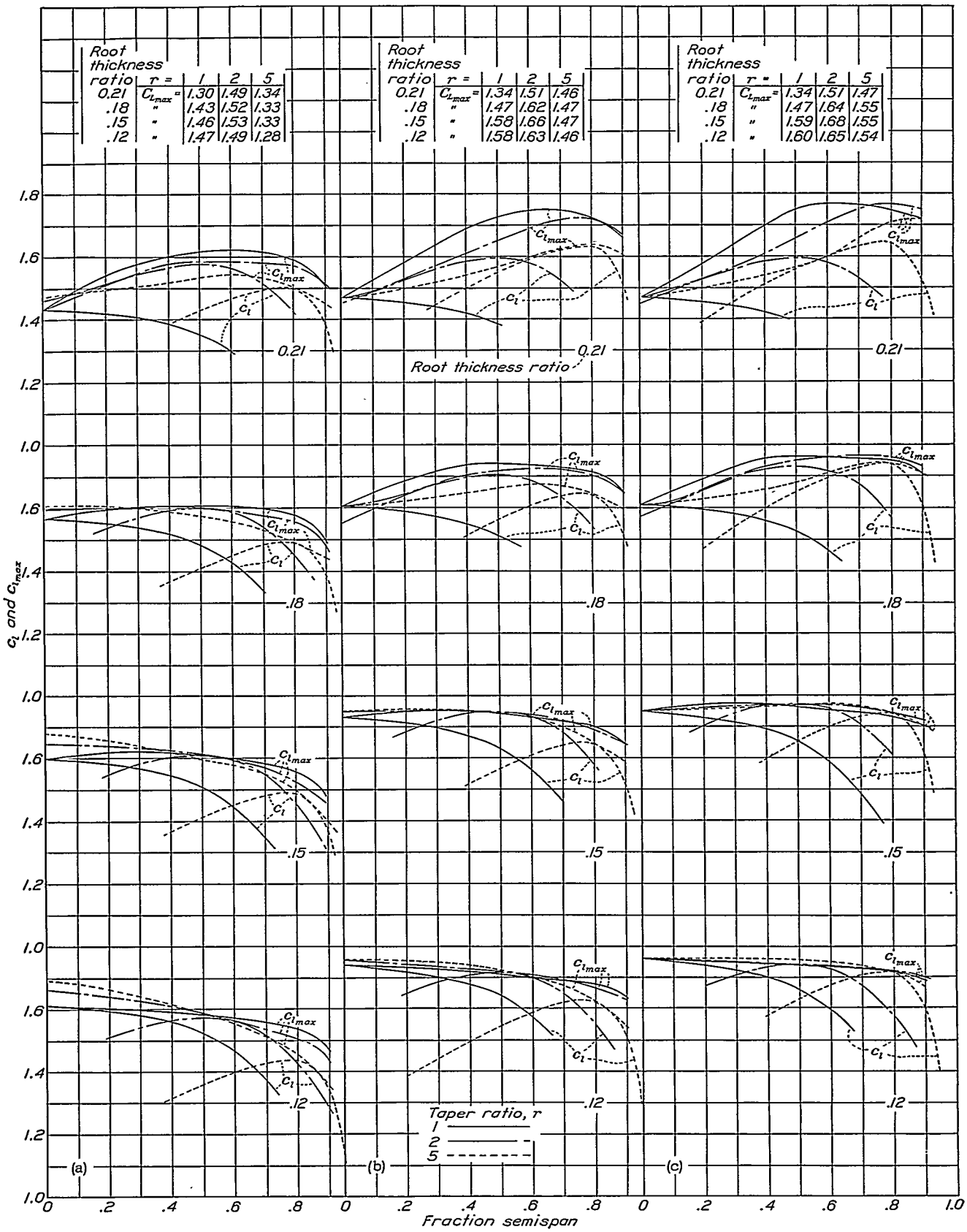

(a) Average Reynolds number, 4,000,000. (b) Average Reynolds number, 8,000,000. (c) Average Reynolds number, 14,000,000.

FIGURE 4.—Distribution of c_l and $c_{l_{max}}$ over semispan. NACA 230 series airfoils; tip thickness ratio, 0.09.

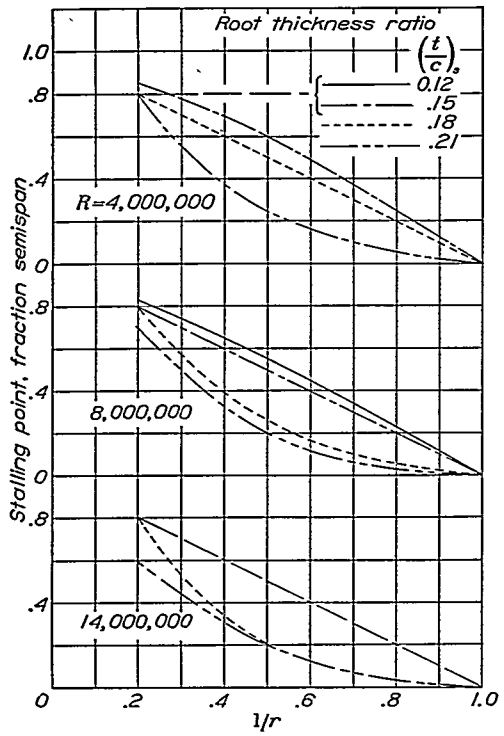

FIGURE 5.—Effect of taper on the location of the stalling point. Tip thickness ratio, 0.09.

The curves of $c_{l_{max}}$ given in figure 4 show the maximum lift coefficients of the individual airfoil sections. For each airfoil section and Reynolds number, $c_{l_{max}}$ was found from

$$c_{l_{max}} = \left(c_{l_{max}}\right)_{std} + \Delta c_{l_{max}}$$

The $\left(c_{l_{max}}\right)_{std}$ values, for the standard effective Reynolds number of 8,200,000 used in variable-density-tunnel tests, were obtained from reference 4. The values of $\Delta c_{l_{max}}$, which correct $c_{l_{max}}$ to the Reynolds number of the particular section, were obtained from reference 5.

The lift coefficients c_l for each section along the span were obtained from figure 2 for a value of C_L that made the c_l curves tangent to the $c_{l_{max}}$ curves. At the point of tangency, c_l reaches the maximum possible value and stalling should begin. This procedure is equivalent to using the section angles of attack and is more convenient. The corresponding wing lift coefficient is the value of effective maximum lift coefficient, or $C_{L_{max}}$. The values of c_l are given in figure 4 only for an aspect ratio of 6 because c_l varies inappreciably in the range of aspect ratios (6 to 9) commonly used in design. The stalling-point data given in figure 4 are

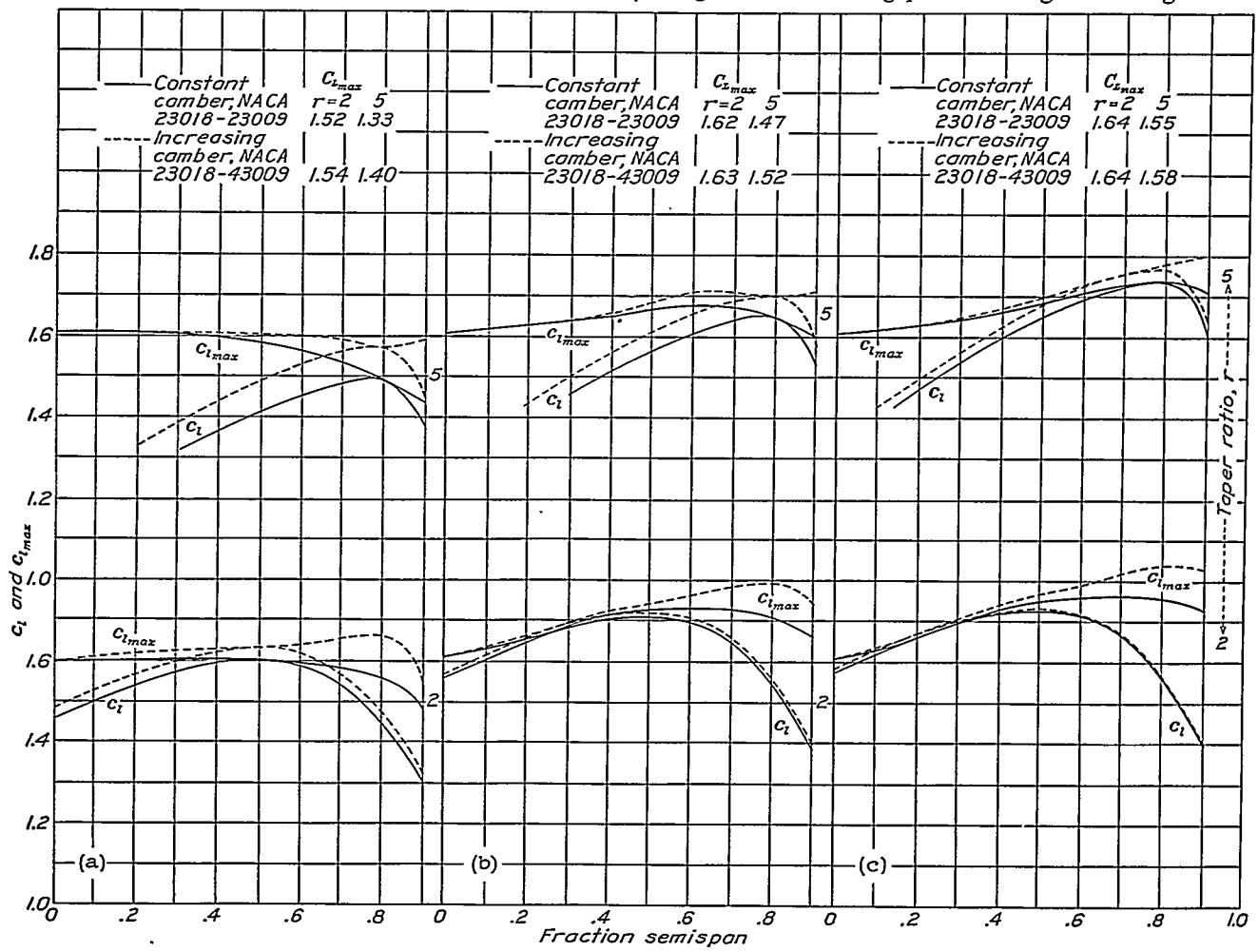

(a) Average Reynolds number, 4,000,000. (b) Average Reynolds number, 8,000,000. (c) Average Reynolds number, 14,000,000.

FIGURE 6.—Effect of linear percentage camber increase from root to tip.

summarized in figure 5, which shows the variation of the stalling point with $1/r$. Although only the NACA 230 series airfoil sections were used, the location of the stalling point should be nearly the same for commonly used sections.

The rate at which the c_l and the $c_{l_{max}}$ curves separate is believed to be an added indication of the nature of the stall. The difference between the curves is the margin between the actual lift coefficient and the stalling lift coefficient of the sections. Where the margin is small, a slight disturbance may produce a stall over a large portion of the wing. As shown in figure 4 (b), for example, conditions for the wing with a taper ratio of 5 and a root thickness ratio of 0.21 are probably less favorable than for the wing with a taper ratio of 5 and a root thickness ratio of 0.15, although the initial stalling point of the second wing is not so far outboard as that of the first.

The rectangular wing (taper ratio of 1) is conceded to have the most desirable stalling characteristics. As may be observed from figure 4, the initial stalling takes place at the center of the span and the c_l and the $c_{l_{max}}$ curves separate fairly rapidly. Increasing taper tends to move the stalling point progressively outboard and to decrease the stalling margin of most of the rest of the wing. The relative importance of these two effects is unknown and both should be kept in mind when considering stalling characteristics.

The stalling characteristics of tapered wings should be improved by moving the stalling point inboard and by increasing the margin between the c_l and the $c_{l_{max}}$ curves over the outer part of the wing. Several methods that have been suggested of moving the stalling point inboard are the use of: camber increase of the airfoil section from center to tips, washout, sharp leading edges at the center, and leading-edge slots.

The effect of a linear increase of camber on the c_l margin is shown in figure 6 for a typical thickness ratio, two taper ratios, and three Reynolds numbers. As will be observed, the increase of camber produces an increase of $c_{l_{max}}$ from root to tip. The camber was limited to 4 percent at the tips because a greater increase of camber would produce no greater increase of $c_{l_{max}}$. No aerodynamic washout is present; that is, the zero-lift directions of the root and the tip sections are parallel. As the angle of zero lift of the NACA

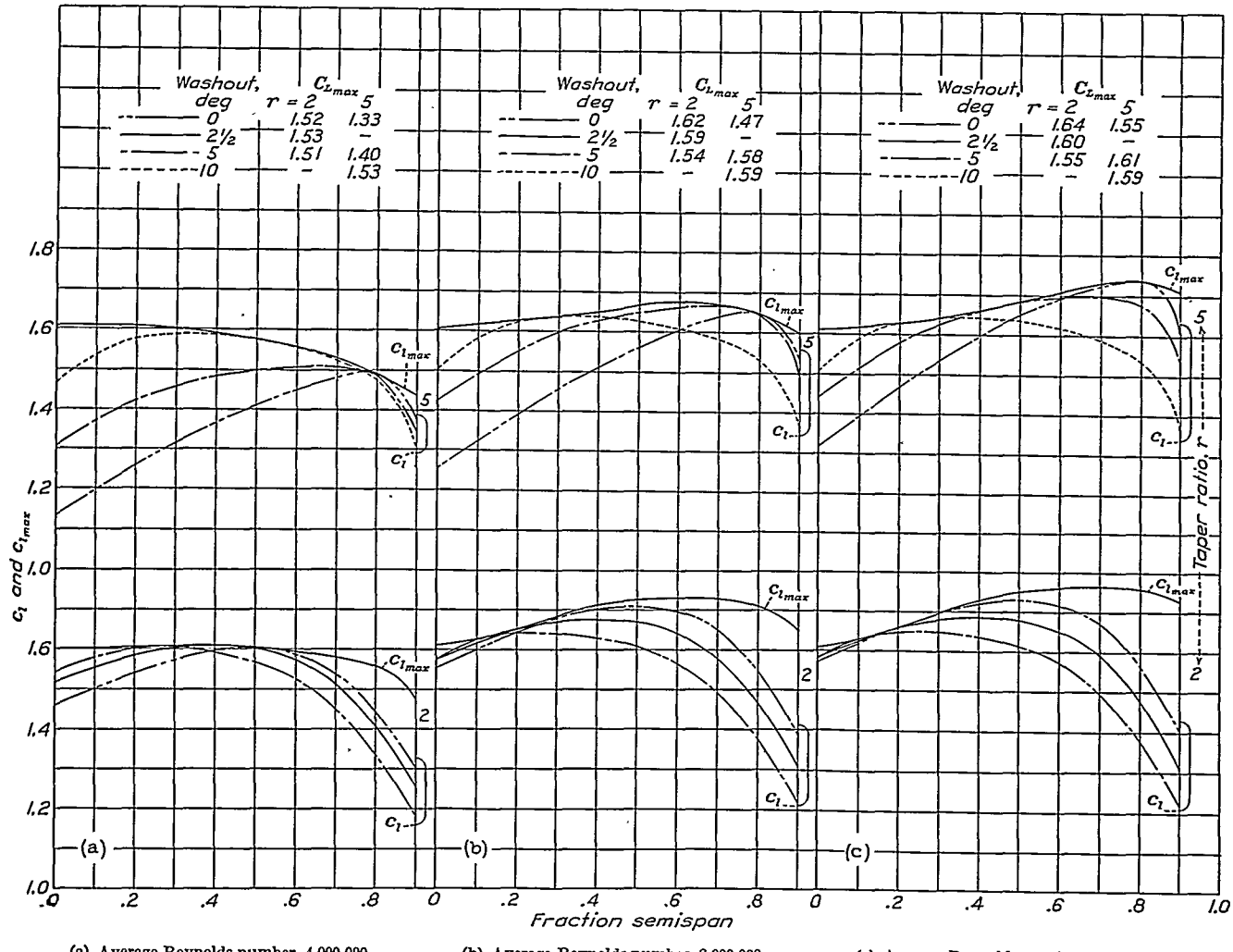

(a) Average Reynolds number, 4,000,000. (b) Average Reynolds number, 8,000,000. (c) Average Reynolds number, 14,000,000.

FIGURE 7.—Effect of linear washout. Constant camber; NACA 23018–23009 sections.

43009 is −2.4° and that of the NACA 23018 is −1.2°, a geometric washout of 1.2° must be used to produce zero aerodynamic washout.

The effect of linear aerodynamic washout on the c_l margin is shown in figure 7 for the same conditions used for the wings with camber increase. The $c_{l_{max}}$ values are the same as for the cases with constant camber but values from figures 2 and 3 have been combined to obtain the tangent c_l curves for the given angles of aerodynamic washout. The effect of combined increase of camber and washout may be inferred from the curves showing the separate effects (figs. 6 and 7).

The two methods considered thus far of moving the initial stall inboard consist in making a gradual change of margin. An abrupt change caused by the effect on $c_{l_{max}}$ may be obtained by the use of sharp leading edges at the center or by leading-edge slots at the tip. Although the first method reduces $c_{l_{max}}$ at the center and the second increases it at the tips, the two methods are similar in application and in underlying principle. An illustration of the effect of a sharp leading edge in combination with washout is given in figure 8. The angle of washout was taken as 1¼°. The use of a sharp leading edge was assumed in order to make the margin at seven-tenths of the semispan the same as the case of 2½° washout of figure 7 (b). The value of $c_{l_{max}}$ is assumed to be reduced over a central region to the value of c_l. Data on the effect of sharp leading edges on the maximum lift coefficient may be found in references 6 and 7. The data given in reference 8 on the effect of protuberances may also be of assistance in determining how to produce a desired decrease in $c_{l_{max}}$.

Figure 8 also provides a comparison of alternate installations of sharp leading edges and of leading-edge slots on the same wing. It is of interest to note that the slot need not extend to the wing tip. The effect of a leading-edge slot is illustrated for a high taper ratio in figure 9. The slot for this case extends from inboard of the stalling point of the unslotted wing to the tip.

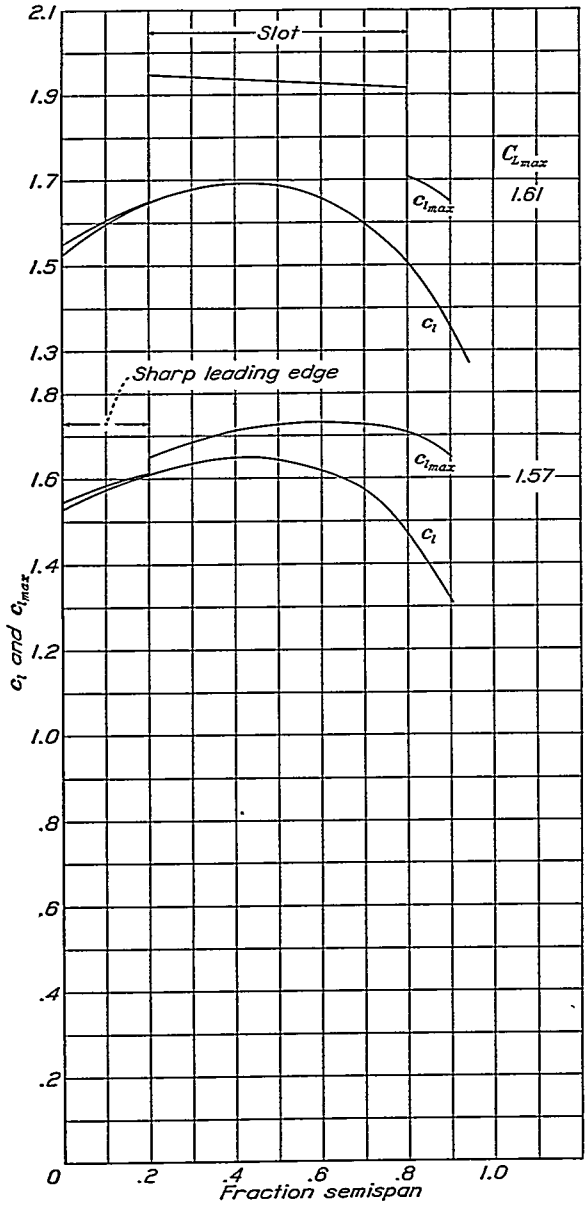

FIGURE 8.—Distribution of c_l and $c_{l_{max}}$ for sharp leading edge and slots on wing of r=2. Average Reynolds number, 8,000,000; washout, 1¼°; constant camber; NACA 23018–23009 sections.

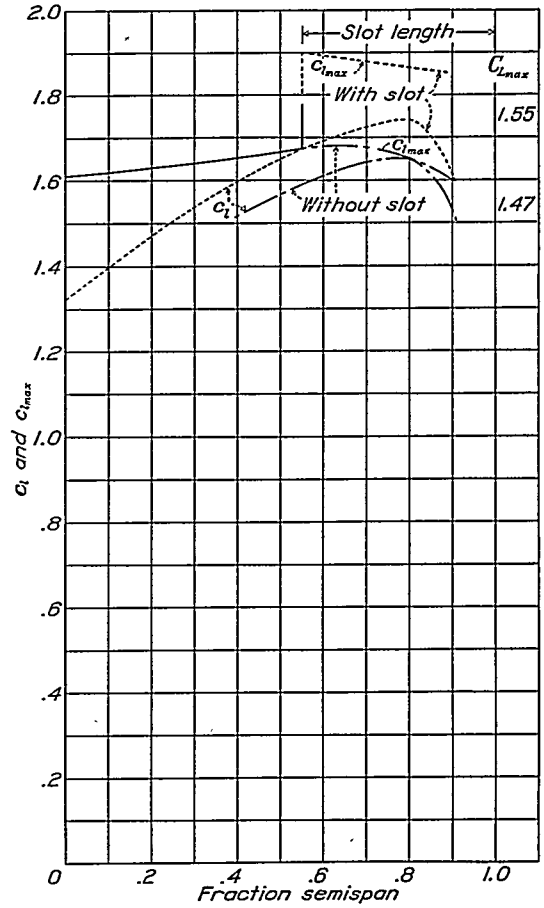

FIGURE 9.—Effect of a slot on wing of r=5. Average Reynolds number, 8,000,000; constant camber; NACA 23018–23009 sections.

Arbitrary $c_{l_{max}}$ values were assumed for the slotted sections for figures 8 and 9 but equal or larger values should be obtainable in practice. Slot lengths necessary for any of the basic wings may be found by observation of figure 4.

It is not so generally appreciated that, under certain conditions, the use of a straight center portion may reduce the tip-stalling tendencies of tapered wings because of its effect on the $c_{l_{max}}$ and c_l curves. The effect of straight center sections is illustrated in figure 10. The wings shown, except for the straight inner 20 percent of the semispan, correspond to two of the wings shown in figure 4 (b). The distribution of the additional lift coefficient may be quickly found for such wings from reference 1, page 8.

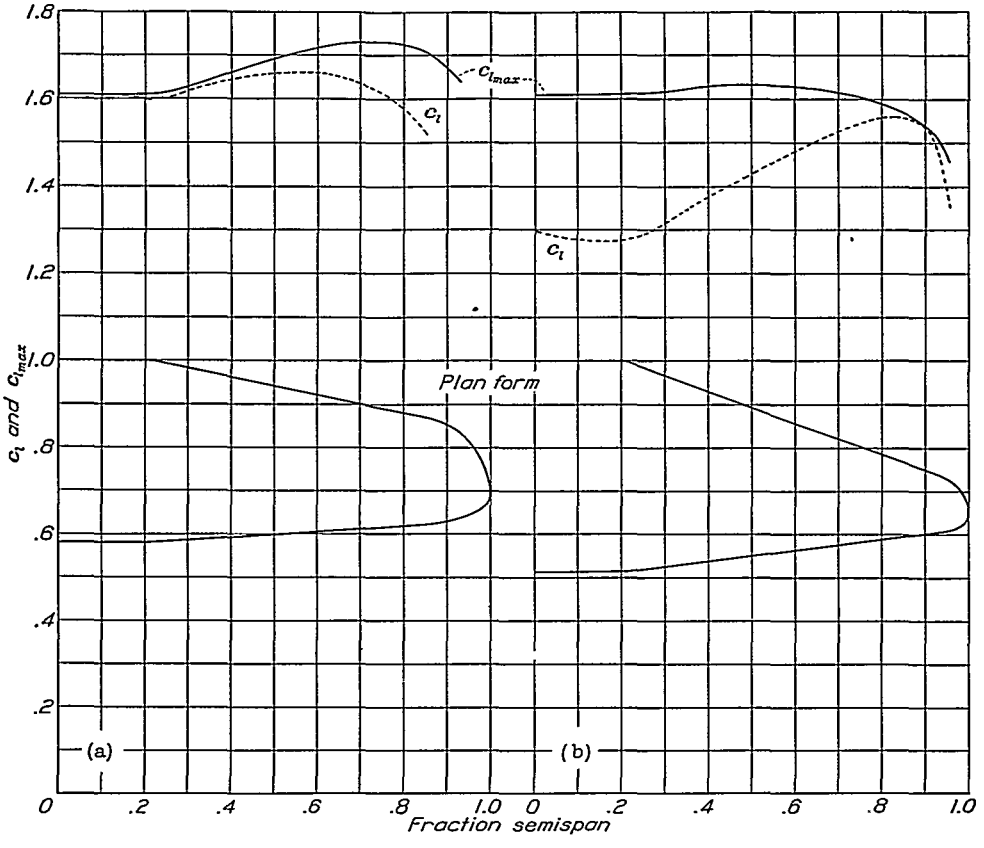

(a) Taper ratio, 2. (b) Taper ratio, 5.

FIGURE 10.—Wings with straight center sections. Average Reynolds number, 8,000,000; constant camber; NACA 23018–23009 sections.

EFFECT ON MAXIMUM LIFT AND DRAG

The various means of increasing the tip margin and moving the stalling point inward usually affect the maximum lift coefficient and the drag coefficient. The magnitude of the effect on the maximum lift coefficient may be determined as previously mentioned. The effect on the drag coefficient in the cruising range may be on either the profile-drag coefficient, the induced-drag coefficient, or both, depending on the device used. The use of increase in camber with zero aerodynamic twist produces an increase only in the profile-drag coefficient. The increase will be small, however, as a camber increase from 2 to 4 percent produces an increase in the minimum section drag coefficient of only 0.0002.

The use of washout affects both the profile-drag and the induced-drag coefficients. The effect on the profile-drag coefficient at low wing lift coefficients will be small; for example, washout of 5° is calculated to increase C_{D_0} for a C_L of zero only 0.0001. The effect on the induced-drag coefficient may be large. For washout of 5° at a C_L of 0.2, the increase of C_{D_i} will be of the order of 0.0010 for a taper ratio of 2. Figure 11 gives the data for estimating the change in the induced-drag coefficient ΔC_{D_i} produced by linear washout up to 6°. The values of ΔC_{D_i} were computed from reference 1.

The value of ΔC_{D_i} may be expressed in the form

$$\Delta C_{D_i}=k_1\epsilon^2+k_2 C_L\epsilon$$

where k_1 and k_2 are constants depending on the taper ratio and the aspect ratio. Thus, at $C_L=0$, ΔC_{D_i} increases as the square of the washout angle. As C_L is increased from zero, a further increment of induced-drag coefficient is added, which is proportional to C_L and ϵ and has a sign depending on the taper ratio. Figure 11 shows this effect; ΔC_{D_i} increases as C_L increases for $r=5$ but decreases for $r=1$.

Sharp leading edges and properly designed closable slots on wings of conventional construction should have a negligible effect on the profile-drag coefficient in the cruising range. Fixed slots will increase the profile-drag coefficient by an amount depending on the particular installation. The increase may be calculated if the increments Δc_{d_0} added to the section profile-drag coefficients are known. For a wing with

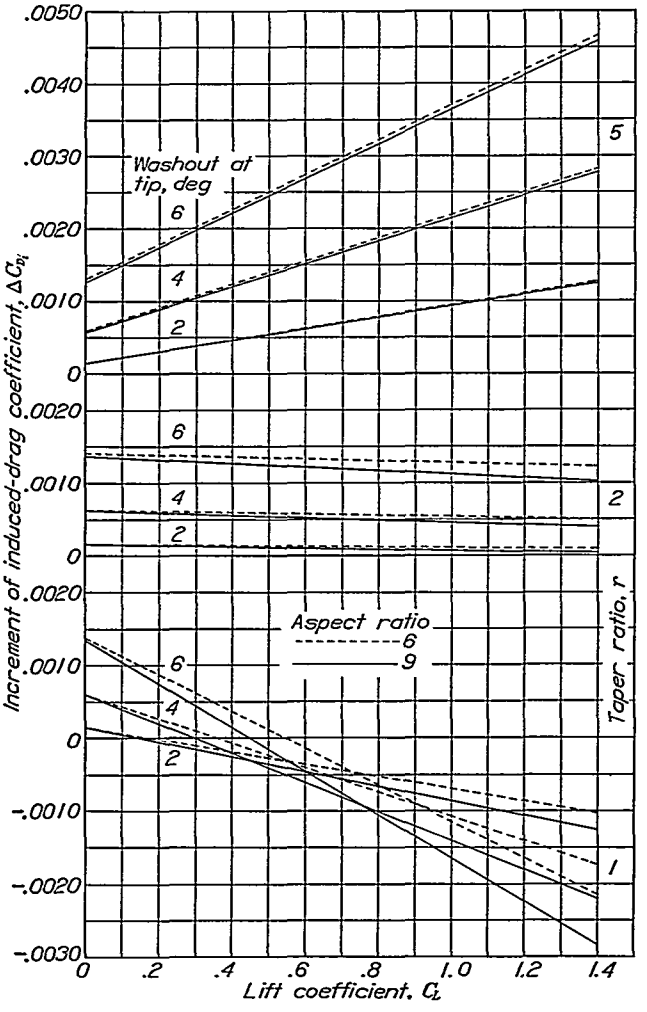

FIGURE 11.—Change in induced-drag coefficient caused by linear washout.

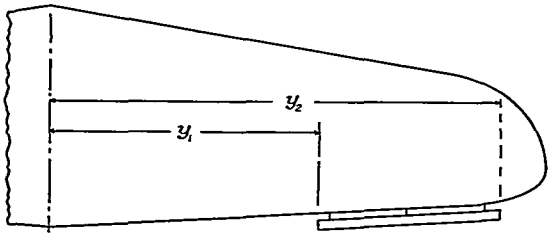

FIGURE 12.—Wing with a slot.

a slot (fig. 12), the increase in the wing profile-drag coefficient based on the wing area S would be

$$\Delta C_{D_0}=\frac{2}{S}\int_{y_1}^{y_2}\Delta c_{d_0} c\,dy$$

where c is the chord at any distance from the center. The value of ΔC_{D_0} can be most conveniently obtained from the area under a curve of Δc_{d_0} c plotted against the semispan. If Δc_{d_0} may be assumed constant with airfoil section and Reynolds number, then ΔC_{D_0} becomes

$$\Delta C_{D_0}=\frac{\Delta S}{S}\Delta c_{d_0}$$

where ΔS is the total wing area behind the slots. To the increment calculated in the foregoing manner, another increment probably should be added because of the effect of the discontinuities at the ends of the slots, but no qualitative data are available on this effect. Values of Δc_{d_0} for a slotted NACA 23012 airfoil are given in reference 9. Considerable variation is shown, the amount depending on the design characteristics, but the value of ΔC_{D_0} for a half-semispan tip slot on a wing with a taper ratio of 2 is estimated to be between 0.0022 and 0.0044. For a wing with a taper ratio of 5, the value of ΔC_{D_0} should fall between 0.0018 and 0.0035 for the same slot length.

DISCUSSION

For convenience in the discussion of the general trends shown by the charts, the wing variables are divided into two groups. One group includes the basic variables—taper ratio, aspect ratio, thickness ratio, and Reynolds number. The other group includes the secondary variables—camber increase, washout, sharp leading edges, and leading-edge slots—which are primarily employed to eliminate poor stalling characteristics resulting from certain combinations of the basic variables.

As expected, the basic characteristic having the greatest effect is taper ratio. In addition to its effect on the theoretical lift-coefficient distribution, taper ratio also affects the $c_{l_{max}}$ distribution along the span by affecting the distribution of thickness ratio and of Reynolds number. The effect of taper ratio on the distribution of thickness ratio, as illustrated in figure 1 for a root thickness ratio of 0.18, shows a large increase in thickness ratio toward the tips as the taper is increased. It may be of interest to note than the t/c distribution is independent of aspect ratio. As the taper ratio is increased, the Reynolds number near the tip is reduced, which results in a reduction of $c_{l_{max}}$ for the most commonly used airfoil sections. The effect is greatest for thin sections and low Reynolds numbers (in the neighborhood of 3,000,000). The combined effects of taper ratio on the thickness ratio and the Reynolds number distribution are such that the values of $c_{l_{max}}$ near the tips are generally decreased as the taper ratio is increased. Also, for all taper ratios, $c_{l_{max}}$ tends to decrease from root to tip for the wings with thin root sections and to increase for the wings with thick root sections.

An increase in aspect ratio tends to flatten out the c_l distribution but, up to the largest value of aspect ratio

covered in the present study, the effect on the stalling point should be relatively small.

With regard to the effect of thickness ratio, figure 5 shows that an increase of root thickness ratio beyond 0.15 causes the stalling point to move inward except for the lowest Reynolds number. The increase of root thickness ratio also tends to reduce the rate at which the c_l and the $c_{l_{max}}$ curves diverge inboard of the initial stalling point (fig. 4). Although a tip thickness ratio of 0.09 was used for all cases, it is common practice to keep the thickness ratio constant for rectangular wings; in that case, $c_{l_{max}}$ would be constant along the semispan. The effect of increasing the tip thickness ratio by a reasonable amount was investigated and was found to have a relatively small effect; the data therefore are not given.

An increase in Reynolds number tends to move the initial stalling point inboard. Figure 5 shows that, with certain combinations of the other variables, the effect may be large. As the Reynolds number is mainly a function of the airplane size, it is apparent that the means of improving the stall of an airplane of one size may be unsatisfactory on an airplane of another size. This difference between large and small airplanes may account for the contradictory stalling behavior observed in flight for airplanes of different size having similar wing plan forms.

As has been previously mentioned, the secondary variables are employed to move the point of the initial stalling toward the center of the wing and to provide a margin between the c_l and the $c_{l_{max}}$ curves near the tip. Aside from the fact that the stalling should start sufficiently far inboard that the pilot will have some warning of the impending loss of rolling stability, either by a change of elevator-control characteristics or by vibration of the tail resulting from the turbulent flow from the wings, nothing definite is known concerning either the optimum point at which stalling should start or of the most desirable amount of margin to be provided near the outer portion of the wing.

For methods that provide a gradual change in the margin, such as washout and camber increase, the margin should probably be equal to or larger than that used in reference 3; that is, the c_l margin should be at least 0.1 at seven-tenths of the semispan. For the case of an abrupt and a large change in maximum lift coefficient, such as produced by slots, conditions will probably be satisfactory if the slots are extended about one-fourth of the semispan to each side of the stalling point of the unslotted wing. More information on this point is needed. It should be appreciated that, under certain conditions, the slots may be located somewhat inboard of the wing tips.

The effect on the location of the stalling point of linear camber increase to the tips is, as shown by figure 6, relatively small. The effects are similar for the three Reynolds numbers. For a taper ratio of 2, there is a slight inward movement of the stalling point accompanied by an increase in margin over the outer part of the wing. Very little change in the initial stalling point or margin occurs for a taper ratio of 5, although the wing maximum lift coefficient appreciably increases. Camber increase therefore appears to be useful only for low taper ratios, where the c_l and the $c_{l_{max}}$ curves remain close together over a considerable portion of the wing span.

Washout, although it is expensive from considerations of drag, offers a very effective means of improving the stalling characteristics of airplanes for which the performance is not the primary consideration. As illustrated in figure 7, washout becomes more effective as the Reynolds number is increased. The value of the wing maximum lift coefficient tends to decrease as the washout is increased for a taper ratio of 2 and to increase for a taper ratio of 5, as would be expected from a consideration of the shape of the curves of lift-coefficient distribution in figure 2.

The effect of washout on the induced drag has already been mentioned; some trends of figure 11, which gives the induced-drag increment resulting from washout, are of interest. It will be observed that, for the rectangular wing above a moderate value of wing lift coefficient, the value of ΔC_{D_i} becomes negative. The value of C_{D_i} will then be less than for the wing with no washout because an elliptical span loading is approached. For the elliptical wing, ΔC_{D_i} does not vary with C_L. For taper ratios more than about 2, ΔC_{D_i} increases with C_L.

The effect of a central sharp leading edge on the c_l margin is shown in figure 8. The margin at seven-tenths of the semispan is the same as for the case of 2½° washout (fig. 7 (b)). Only a small reduction of $c_{l_{max}}$ at the center is required to permit half the washout to be used and there is only a small reduction of $C_{L_{max}}$. The use of camber increase would provide a gain in $C_{L_{max}}$; in fact, a combination of moderate amounts of camber increase, washout, and sharp leading edge was shown in reference 3 to be the most efficient combination of these means. In connection with the use of sharp leading edges, it is important to note that the wing lift coefficient is directly affected by the decrease of $c_{l_{max}}$ caused by the sharp leading edges.

Although the leading-edge slots are superior to sharp leading edges from considerations of wing maximum lift coefficient, they are undoubtedly less advantageous as regards their effect on the drag and from the difficulty of installation. The automatic or closable type of slot should produce no increase of drag, but considerable mechanical complication is involved. The fixed type of slot reduces the mechanical complication but results in an increase of drag and a loss of high speed.

For a given airplane design, the choice of taper ratio

will depend on both aerodynamic and structural factors. The structural advantages of high taper are well known; the stalling problem may, however, be so accentuated by the use of extreme taper that it may be more expedient to reduce the taper than to employ large amounts of washout, camber increase, etc. (See reference 3.) If a choice is to be made between a combination of camber increase and washout and fixed slots, the charts indicate that, for a taper ratio of 5, the high-speed drag would be most affected by camber increase and washout because of the large amount of washout required. For moderate taper ratios, however, camber increase and washout should result in a lower drag increase.

Several observations of the action of tufts on wings have been made with a view to checking the accuracy of the predicted stalling points. Wind-tunnel observations, although they indicate no definite stalling point, agree in showing an outward movement of the stalling region as the taper is increased. Flight tests of a single-engine airplane also showed stalling to start near the predicted point. For multiengine airplanes, however, comparison of the actual with the predicted stalling point becomes complicated because of the effect of the nacelles and the slipstream.

It is appreciated that the present charts do not cover the entire field of possible variables. Other factors, such as sweepback, partial-span flaps, nacelle and fuselage interference, and propeller slipstream, are known to have a considerable influence on the stalling characteristics of a wing. At present, theoretical treatment of these factors is insufficiently advanced for use in the present paper. Because of the importance of these characteristics, it is recommended that experimental and theoretical work be undertaken to study the influence of these factors.

APPLICATION OF CHARTS

Although data for all the possible designs for tapered wings cannot be given it is hoped that enough data have been given to be useful in design. The application of the data is perhaps best illustrated by an example. Consider an airplane with a wing loading of 23 pounds per square foot and a wing having the following characteristics: S/b, 8.3 feet; taper ratio, 3; aspect ratio, 6; root thickness ratio, 0.165; and tip thickness ratio, 0.09. A value of $C_{L_{max}}$ of 1.5 will be assumed, corresponding to a stalling speed of 77 miles per hour. The Reynolds number would then be 6,000,000. By interpolation between the values of $C_{L_{max}}$ given in figures 4 (a) and 4 (b), a value of $C_{L_{max}}$ of 1.48 is computed, which is sufficiently close that no further approximations are required. From figure 5, the stalling point is found by interpolation to be at 0.65 of the semispan; this location is considered unsatisfactory and some means of moving the stalling point inward must be used.

For methods of moving the stalling point inward that provide a gradual increase in margin near the tips, a c_l margin at seven-tenths of the semispan of 0.15 will be considered satisfactory. Although figures 6 (a) and 6 (b) are for a root thickness ratio other than that used in this example, they indicate that camber increase alone is incapable of producing the desired margin. The amount of aerodynamic washout required to give the desired margin is estimated from figure 7 to be about 7° between the root and the tip sections. By extrapolation from figure 11, the increase in the induced-drag coefficient resulting from this amount of washout would be $\Delta C_{D_i}=0.0019$ at a cruising C_L of 0.25. The importance of this drag increase is, of course, dependent on the total airplane drag coefficient. For an airplane with a drag coefficient of 0.02, the use of 7° washout would reduce the cruising speed by approximately 3 percent.

If it is desired to employ only sharp leading edges at the center, their approximate span and the amount that they should reduce the section lift coefficient may be obtained from figure 4. For the example cited, sharp edges having a length of two-tenths of the semispan on each side of the center will probably be satisfactory. In order to provide the specified c_l margin at seven-tenths of the semispan, the sharp leading edges should be designed to reduce by about 0.30 the value of section lift coefficients of the sections where they are applied. For these conditions, the wing maximum lift coefficient should be reduced by 10 percent and the minimum speed increased by 5 percent.

On the basis that leading-edge slots, if employed, should extend one-fourth of the semispan to each side of the initial stalling point for the wing without the slots, the slots for the wing of the example should extend from four-tenths of the semispan to nine-tenths of the semispan, affecting approximately 40 percent of the wing area. With this slot, the wing maximum lift coefficient would be increased by about 4 percent. A good installation of a closable slot should cause only a small drag increase. For some of the better forms of fixed slots, reference 9 gives values of Δc_{d_0} less than 0.0080. For these fixed slots, the airplane drag coefficient would be increased by 0.0032. For the airplane previously considered, this drag increase would correspond to a loss of speed of 5 percent.

As previously mentioned, the most efficient arrangement for providing the desired margin against tip stalling probably is a combination of several of the foregoing methods. One possible arrangement consists in a variation of the airfoil section from the NACA 23016.5 at the root to the NACA 43009 at the tip with a linear variation of camber and thickness. Aerodynamic washout of 3° is employed and a sharp leading edge is applied over the middle 10 percent of the wing span. The c_l and the $c_{l_{max}}$ curves for this arrangement are given in figure 13.

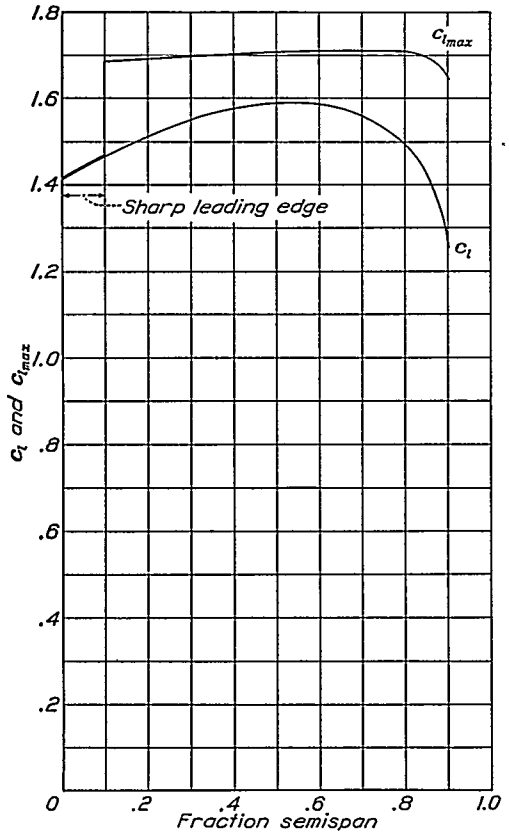

FIGURE 13.—Illustration of combined use of washout, camber increase, and sharp leading edge. Washout, 3°; NACA 23016.5-43009 sections; average Reynolds number, 6,000,000; taper ratio, 3; $C_{L_{max}}$, 1.51.

When combinations of variables are to be used, $c_{l_{max}}$, $c_{l_{a1}}$, and c_{l_b} should probably be plotted for the particular set of conditions involved. Such plots can be made by interpolation of the material presented herein or, more accurately, by the method of reference 2. The procedure followed in the development of the wing of the previous paragraph follows: From the value of $c_{l_{max}}$ at seven-tenths of the semispan, the required margin of 0.15 was subtracted, which determined the value of c_l. For this spanwise station, c_{l_a} was then found from $c_{l_a}=c_l-c_{l_b}$. The ratio $c_{l_a}/c_{l_{a1}}$ at seven-tenths of the semispan determined the factor $C_{L_{max}}$ by which the ordinates of the $c_{l_{a1}}$ curve were multiplied to obtain the c_{l_a} curve. The c_l curve was obtained by combining the c_{l_a} curve thus found with the c_{l_b} curve. The lift decrement of the required sharp leading edges was then determined by the amount required to reduce $c_{l_{max}}$ to c_l, as shown in figure 13.

The increase in C_{D_0} resulting from camber increase and washout will be negligible. The increase in C_{D_i} is small and may be found for the desired taper ratio by a cross plot from figure 11. At a cruising C_L of 0.25, ΔC_{D_i} was found to be 0.0004, which corresponds to a loss of speed of less than 1 percent for the airplane previously considered.

NATIONAL ADVISORY COMMITTEE FOR AERONAUTICS,
LANGLEY MEMORIAL AERONAUTICAL LABORATORY,
LANGLEY FIELD, VA., *January 18, 1940.*

REFERENCES

1. Anderson, Raymond F.: Determination of the Characteristics of Tapered Wings. Rep. No. 572, NACA, 1936.
2. Anderson, Raymond F.: The Experimental and Calculated Characteristics of 22 Tapered Wings. Rep. No. 627, NACA, 1938.
3. Anderson, Raymond F.: A Comparison of Several Tapered Wings Designed to Avoid Tip Stalling. T. N. No. 713, NACA, 1939.
4. Jacobs, Eastman N., Pinkerton, Robert M., and Greenberg, Harry: Tests of Related Forward-Camber Airfoils in the Variable-Density Wind Tunnel. Rep. No. 610, NACA, 1937.
5. Jacobs, Eastman N., and Sherman, Albert: Airfoil Section Characteristics as Affected by Variations of the Reynolds Number. Rep. No. 586, NACA, 1937.
6. Jacobs, Eastman N.: Characteristics of Two Sharp-Nosed Airfoils Having Reduced Spinning Tendencies. T. N. No. 416, NACA, 1932.
7. Weick, Fred E., and Scudder, Nathan F.: The Effect on Lift, Drag, and Spinning Characteristics of Sharp Leading Edges on Airplane Wings. T. N. No. 447, NACA, 1933.
8. Jacobs, Eastman N.: Airfoil Section Characteristics as Affected by Protuberances. Rep. No. 446, NACA, 1932.
9. Bamber, M. J.: Wind-Tunnel Tests of Several Forms of Fixed Wing Slot in Combination with a Slotted Flap on an NACA 23012 Airfoil. T. N. No. 702, NACA, 1939.

AERONAUTIC SYMBOLS

1. FUNDAMENTAL AND DERIVED UNITS

	Symbol	Metric		English	
		Unit	Abbreviation	Unit	Abbreviation
Length	l	meter	m	foot (or mile)	ft (or mi)
Time	t	second	s	second (or hour)	sec (or hr)
Force	F	weight of 1 kilogram	kg	weight of 1 pound	lb
Power	P	horsepower (metric)		horsepower	hp
Speed	V	kilometers per hour	kph	miles per hour	mph
		meters per second	mps	feet per second	fps

2. GENERAL SYMBOLS

W Weight$=mg$

g Standard acceleration of gravity$=9.80665$ m/s^2 or 32.1740 ft/sec^2

m Mass$=\frac{W}{g}$

I Moment of inertia$=mk^2$. (Indicate axis of radius of gyration k by proper subscript.)

μ Coefficient of viscosity

ν Kinematic viscosity

ρ Density (mass per unit volume)

Standard density of dry air, 0.12497 kg-m^{-4}-s^2 at 15° C and 760 mm; or 0.002378 lb-ft^{-4} sec^2

Specific weight of "standard" air, 1.2255 kg/m^3 or 0.07651 lb/cu ft

3. AERODYNAMIC SYMBOLS

S Area

S_w Area of wing

G Gap

b Span

c Chord

A Aspect ratio, $\frac{b^2}{S}$

V True air speed

q Dynamic pressure, $\frac{1}{2}\rho V^2$

L Lift, absolute coefficient $C_L=\frac{L}{qS}$

D Drag, absolute coefficient $C_D=\frac{D}{qS}$

D_0 Profile drag, absolute coefficient $C_{D_0}=\frac{D_0}{qS}$

D_i Induced drag, absolute coefficient $C_{D_i}=\frac{D_i}{qS}$

D_p Parasite drag, absolute coefficient $C_{D_p}=\frac{D_p}{qS}$

C Cross-wind force, absolute coefficient $C_C=\frac{C}{qS}$

i_w Angle of setting of wings (relative to thrust line)

i_t Angle of stabilizer setting (relative to thrust line)

Q Resultant moment

Ω Resultant angular velocity

R Reynolds number, $\rho\frac{Vl}{\mu}$ where l is a linear dimension (e.g., for an airfoil of 1.0 ft chord, 100 mph, standard pressure at 15° C, the corresponding Reynolds number is 935,400; or for an airfoil of 1.0 m chord, 100 mps, the corresponding Reynolds number is 6,865,000)

α Angle of attack

ϵ Angle of downwash

α_0 Angle of attack, infinite aspect ratio

α_i Angle of attack, induced

α_a Angle of attack, absolute (measured from zero-lift position)

γ Flight-path angle

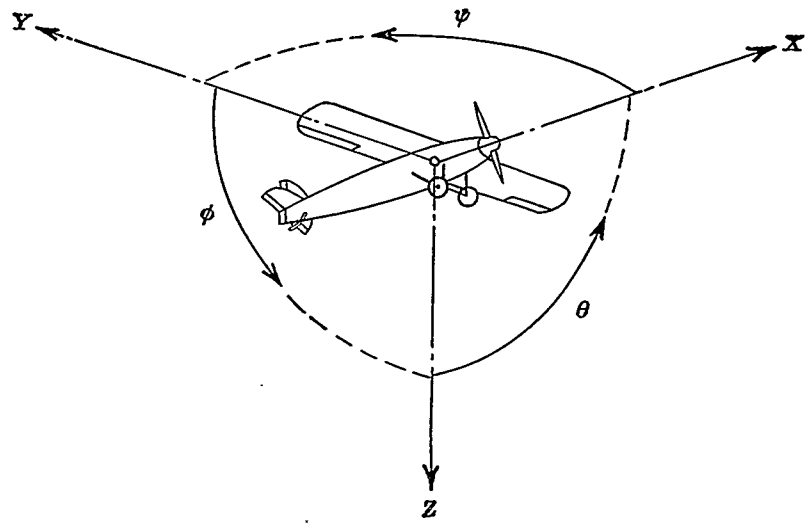

Positive directions of axes and angles (forces and moments) are shown by arrows

Axis		Force (parallel to axis) symbol	Moment about axis			Angle		Velocities	
Designation	Symbol		Designation	Symbol	Positive direction	Designation	Symbol	Linear (component along axis)	Angular
Longitudinal	X	X	Rolling	L	$Y \longrightarrow Z$	Roll	ϕ	u	p
Lateral	Y	Y	Pitching	M	$Z \longrightarrow X$	Pitch	θ	v	q
Normal	Z	Z	Yawing	N	$X \longrightarrow Y$	Yaw	ψ	w	r

Absolute coefficients of moment

$C_l = \frac{L}{qbS}$ (rolling) $\quad C_m = \frac{M}{qcS}$ (pitching) $\quad C_n = \frac{N}{qbS}$ (yawing)

Angle of set of control surface (relative to neutral position), δ. (Indicate surface by proper subscript.)

4. PROPELLER SYMBOLS

D, Diameter

p, Geometric pitch

p/D, Pitch ratio

V', Inflow velocity

V_s, Slipstream velocity

T, Thrust, absolute coefficient $C_T = \frac{T}{\rho n^2 D^4}$

Q, Torque, absolute coefficient $C_Q = \frac{Q}{\rho n^2 D^5}$

P, Power, absolute coefficient $C_P = \frac{P}{\rho n^3 D^5}$

C_s, Speed-power coefficient $= \sqrt[5]{\frac{\rho V^5}{P n^2}}$

η, Efficiency

n, Revolutions per second, r.p.s.

Φ, Effective helix angle $= \tan^{-1}\left(\frac{V}{2\pi r n}\right)$

5. NUMERICAL RELATIONS

1 hp.=76.04 kg-m/s=550 ft-lb./sec.
1 metric horsepower=1.0132 hp.
1 m.p.h.=0.4470 m.p.s.
1 m.p.s.=2.2369 m.p.h.

1 lb.=0.4536 kg.
1 kg=2.2046 lb.
1 mi.=1,609.35 m=5,280 ft.
1 m=3.2808 ft.

○